U.S. Department
of Transportation

**Federal Railroad
Administration**

APPLICATION OF ULTRASONIC PHASED ARRAYS FOR RAIL FLAW INSPECTION

Office of Research and
Development
Washington, DC 20590

DOT/FRA/ORD-06/17

July 2006

REPORT DOCUMENTATION PAGE

Form approved

OMB No. 0704-0188

1. AGENCY USE ONLY *(Leave blank)*	2. REPORT DATE	3. REPORT TYPE AND DATES COVERED
	July 2006	

4. TITLE AND SUBTITLE

Application of Ultrasonic Phased Arrays for Rail Flaw Inspection

5. FUNDING NUMBERS

DTFR53-C-00012
Task Order 209

6. AUTHOR(S)

Greg Garcia, TTCI, and
Jinchi Zhang, Olympus NDT

7. PERFORMING ORGANIZATION NAME(S) AND ADDRESS(ES)

Transportation Technology Center, Inc.
P.O. Box 11130
Pueblo, CO 81001

8. PERFORMING ORGANIZATION REPORT NUMBERS

9. SPONSORING/MONITORING AGENCY NAME(S) AND ADDRESS(ES)

U.S. Department of Transportation
Federal Railroad Administration
Office of Research and Development, MS 20
1120 Vermont Avenue, NW
Washington, DC 20590

10. SPONSORING/MONITORING AGENCY REPORT NUMBER

DOT/FRA/ORD-06/17

11. SUPPLEMENTARY NOTES

12a. DISTRIBUTION/AVAILABILITY STATEMENT

This document is available through National Technical Information Service, Springfield, VA 22161.

12b. DISTRIBUTION CODE

13. ABSTRACT

The average number of Federal Railroad Administration's (FRA) reportable broken rail-related derailments between 1995 and 2005 was approximately 28 annually. The annual property damage resulting from the accidents was approximately $35 million. Programs cosponsored by FRA and the Association of American Railroads are directed at determining causes of internal rail flaws and identifying applicable nondestructive testing (NDT) technologies that can detect the flaws. Through continued efforts from the joint research program, the development and implementation of improved rail metallurgies and maintenance programs are expected to decrease rail flaws. In addition, through increased reliability of flaw detection technologies, a decrease in rail failures and accidents is expected.

The research programs also continue the identification, evaluation, and development of emerging NDT technologies applicable to increased rail flaw detection reliability. Technologies investigated to date include laser-generated ultrasound, low-frequency eddy current, guided ultrasonic waves using magnetostrictive sensors, and ultrasonic phased arrays. Scanning capabilities for phased-array technologies do not currently accommodate real-time dynamic rail inspection at speeds greater than 5 mph. But the method has demonstrated its feasibility for Web, base, and head inspection focused on flaw sizing and characterization. This report provides the results of research sponsored by FRA, through the Transportation Technology Center, Inc., regarding the application of phased-array ultrasonic technology to inspect rail for service induced transverse defects in the head of the rail.

14. SUBJECT TERMS

Phased arrays, transverse defects, electronic scanning, ultrasonic testing, beam steering, linear scanning, circular scanning, time of flight diffraction, nondestructive testing

15. NUMBER OF PAGES

43

16. PRICE CODE

17. SECURITY CLASSIFICATION	18. SECURITY CLASSIFICATION OF THIS PAGE	19. SECURITY CLASSIFICATION OF ABSTRACT	20. LIMITATION OF ABSTRACT
UNCLASSIFIED	UNCLASSIFIED	UNCLASSIFIED	SAR

NSN 7540-01-280-5500

Standard Form 298 (Rec. 2-89)
Prescribed by ANSI/NISO Std. 239.18
298-102

Table of Contents

List of Figures

List of Tables

EXECUTIVE SUMMARY

Programs cosponsored by the Federal Railroad Administration (FRA) and the Association of American Railroads (AAR) are directed at determining causes of internal rail flaws and identifying applicable nondestructive testing (NDT) technologies that can detect the flaws. Through continued efforts from the joint research program, the development and implementation of improved rail metallurgies and maintenance programs are expected to decrease rail flaws. In addition, through increased reliability of flaw detection technologies, a decrease in rail failures/accidents is expected.

Accomplishments of the Rail Flaw Detection Program include implementation of a flaw growth study by Transportation Technology Center, Inc. (TTCI) at the Transportation Technology Center's (TTC) Facility for Accelerated Service Testing (FAST) and the development of the Rail Defect Test Facility (RDTF). RDTF provides a test bed for detector car system evaluations and NDT technology development. Service flaw characterization and NDT technology scanning and development are also being performed to gain better understanding of flaw detection in general.

Phase I of this study determined that the ultrasonic phased-array (PA) technology was feasible for use in detection of transverse defects (TDs). The study showed that by using a linear array approach, PA technology was capable of sizing the TD by providing a fairly accurate interrogation of the flaw size across the railhead from gage to field. Phase II took this approach a step further by researching which PA probe technology would be the most applicable to railhead inspection for the purpose of performing flaw sizing, in the field, from the railhead's side. Lastly, Phase IIA allowed the technology to be set up in a field environment at FAST while monitoring TDs during train operations.

1.0 Introduction

The average number of FRA reportable broken rail-related derailments between 1995 and 2005 was approximately 28 annually. The annual property damage resulting from the accidents was approximately $35 million (1). Programs cosponsored by FRA and AAR through TTCI are directed at determining causes of internal rail flaws and identifying applicable NDT technologies that can detect the flaws. Through continued efforts from the joint research program, the development and implementation of improved rail metallurgies and maintenance programs are expected to decrease rail flaws. In addition, through increased reliability of flaw detection technologies, a decrease in rail failures/accidents is expected.

Accomplishments of the Rail Flaw Detection Program include implementation of a flaw growth study at FAST and the development of RDTF. RDTF provides a test bed for detector car system evaluations and NDT technology development. Service flaw characterization and NDT technology scanning and development are also being performed to gain better understanding of flaw detection in general.

This report provides the results obtained during a feasibility study of PA ultrasonic approaches to inspect the head of the rail for TDs. The report also documents the results obtained in determining appropriate wedge and inspection angles to reliably size TDs in the railhead.

A railhead TD is a progressive fracture containing an internal transverse separation of the rail material that may or may not be exposed to the outside surface of the railhead. Committee-4 Rail, Subcommittee 8–Nondestructive Testing of Rail, of the American Railway Engineering and Maintenance of Way Association (AREMA) has developed a "Draft Rail Defect Manual," which is currently under review by the committee. This manual identifies the following defects as typical TDs found in the head of rail under North American rail service operations (2).

- Detail Fracture (Figure 1)—A progressive fracture that typically originates from a separation close to the running surface of the railhead. This separation turns down and progresses transversely at right angles to the rail's running surface. The defect is usually associated with a horizontal separation that grows parallel to the railhead running surface known as a shell.

Figure 1. Detail Fracture in the Head of a Rail

- Compound Fissure (Figure 2)—A progressive fracture occurring in the head of the rail that originates as a horizontal separation that turns up or down, or in both directions, to form a transverse separation substantially at right angles to the running surface. Compound fissures may include multiple horizontal or vertical planes.

Figure 2. Compound Fissure in the Head of a Rail

- Transverse Fissure (Figure 3)—A progressive crosswise fracture originating from a center or nucleus located internally in the railhead and propagating outward substantially at right angles to the rail's running surface.

Figure 3. Transverse Fissure in the Head of a Rail

- Engine Burn Fracture (Figure 4)—A progressive fracture in the head of the rail that initiates from overheating generated by slipping locomotive wheels. Rapid cooling results in thermal cracks. Its appearance in track is of a round or oval area with slivers from metal flow with the metal flattened or separated just below the surface. Usually the fatigue generated by the engine burn propagates at right angles to the running surface, but this may occur in several directions into the rail.

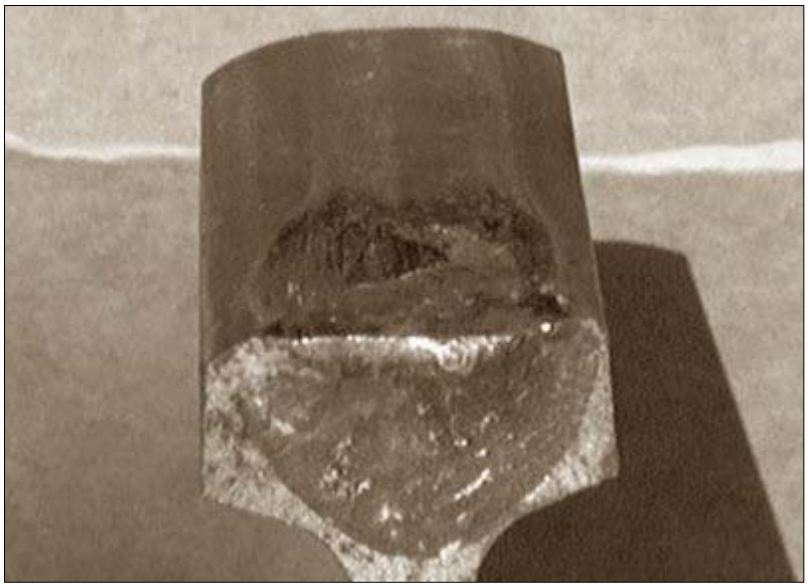

Figure 4. Engine Burn Fracture in the Head of a Rail

- Welded Burn Fracture (Figure 5)—A progressive fracture in the head of the rail that initiates from an inclusion or stress crack resulting from a weld repair rail re-surfacing. The defect will typically initiate at the interface between the weld filler metal and parent material of the rail section. The flaw will progress transversely into the railhead and may not show any visible evidence that a TD is present until the defect breaks out at the railhead surface.

Figure 5. Welded Burn Fracture in the Head of a Rail

Research into applying PA ultrasonic approaches to more reliably size TDs in the field is being performed to increase the level of safety during train operations. Implementation of PA approaches is expected to provide real-time, in-depth characterization of the internal condition of the rail to include the size of flaws detected.

PA technology is applied by electronically modifying the characteristics of acoustic probes used in ultrasonic or eddy current inspections. Modifications of the probes are performed by introducing time shifts in the signals sent to and received from individual elements placed into an array probe. By using specially designed hardware and software, TTCI expects that applicable ultrasonic techniques can be developed and used for rail flaw detection and sizing of railhead TDs using the PA approach.

2.0 Objectives

The primary objective of the FRA-sponsored Rail Flaw Detection Research Program is to improve the reliability and safety of rail operations by developing improved rail flaw detection methods. FRA- and AAR-sponsored efforts at TTC have included the following areas of research:

- Defect Growth: The monitoring of selected internal railhead flaws at FAST. Flaw growth monitoring is performed to identify and understand those factors that contribute to flaw growth and to quantify their effect on growth rate.
- Defect Detection: This effort includes the evaluation of rail flaw detection systems at RDTF. The evaluations are designed to provide insight and understanding into the strengths and limitations of detection systems.
- Service Flaw Characterization: The evaluation of rail service failures is performed to identify rail, flaw, and environmental attributes that may contribute to not detecting rail flaws.
- NDT Technology Investigation: This research focuses on identifying, developing, and/or evaluating NDT technologies for possible use in rail flaw detection.

This report provides background and results of research directed at applying PA ultrasonic approaches to the in-service inspection of rail. TTCI expects that by implementing PA technology to inspect rail, a reliable means of sizing flaws detected in rail can be achieved.

3.0 Procedures

Two phases of research have been performed as part of the program to determine how PA ultrasonic technology can be applied towards the inspection of rail in service. The PA research effort has been performed in conjunction with RD Tech/Olympus NDT, a manufacturer and supplier of ultrasonic and eddy current PA systems. The following paragraphs describe the PA approach used in this project.

A PA approach for rail flaw detection and sizing performed by TTCI under FRA sponsorship has been focused on sizing TDs located in the railhead. The PA process evaluated during this research effort uses an electronic scanning method of transmitting and receiving ultrasonic energy from various locations of the railhead. Electronic scanning is the ability to move an ultrasonic beam electronically along one axis of the array without any mechanical movement. The movement is performed by time multiplexing the active elements. Beam movement depends on probe geometry and can be either linear scanning or circular scanning (3). In this case, linear scanning was used.

PA technology produces certain beam characteristics by time shifting the pulsing and receiving of each array element. These characteristics include beam focusing and skewing to change the angle of incidence (the angle that the sound waves will propagate through the inspection medium). During this effort, detection and sizing were performed by comparing results from PA and conventional probes against each other. This PA application used an active group of 8 elements along 2 transducers of 60 elements, similar to the 16 element setup shown in Figure 6.

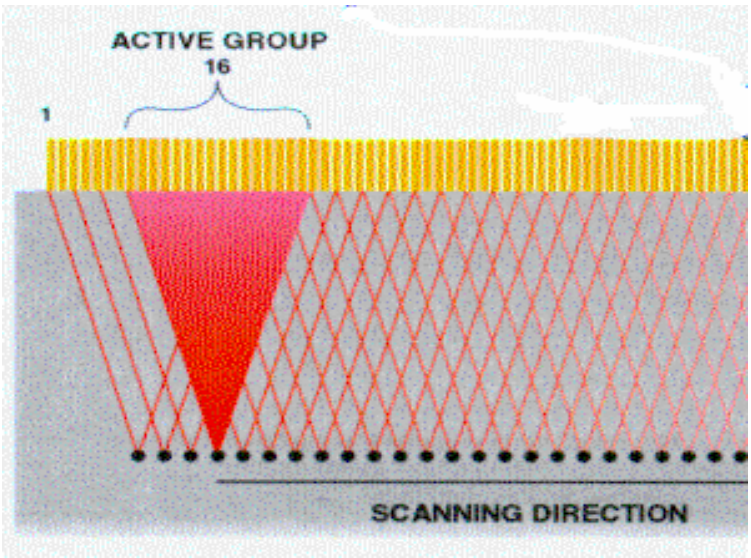

Figure 6. Linear Electronic Scanning

Inspection using the 60-element probe technique uses 2 PA transducers containing 60 elements each. A larger number of elements within the transducer will be evaluated later to optimize the application. For simplicity, the 60-element probes were used for this study. The transducers were applied in the mode to transmit and receive. So if a TD is not present, then the transmitted signal will not return back to the probe given that a reflective surface (impedance mismatch) will not allow the signal to be reflected back to the probe.

During the evaluation of the rail samples, using the conventional probe approach, a transducer that produces a total beam angle of 13 degrees for the 5-MHz probe and 28 degrees for the 2.25-MHz probe was incorporated to increase the probability of hitting the defect. This approach works well to detect the flaws but demonstrates very little in the area of sizing capability. The beam spread is the primary reason for the decrease in sizing sensitivity. The deeper the beam propagates into the railhead, the larger the area of coverage becomes since the area of coverage increases, but the amount of energy focused at a given area decreases the deeper the beam penetrates into the rail. This phenomenon decreases the probability of both detecting and accurately sizing a flaw, as Figure 7 shows.

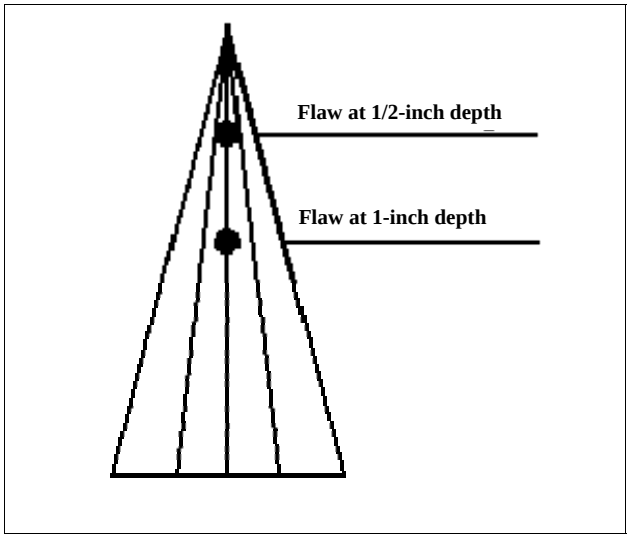

Figure 7. Sketch Showing a Decrease in Sizing Sensitivity Due to Beam Spread

One advantage of using PA technology is the ability to focus an ultrasonic beam. By sweeping a focused beam all along the flaw, sizing of the transverse length of the flaw can be performed. The way this technique was applied was by setting two PA transducers along the railhead as Figure 8 shows and then recording the data. The electronic scan (PA) using the focused beam approach sweeps the flaw. This technique uses a probe with a wedge angle of 33.7 degrees that separates the rail width into many small zones of approximately 0.048 inch (1.2 mm). By incorporating several focused beams along the flaw, each zone that reflects off of the flaw and back to the probe is counted, allowing for increased sensitivity in sizing the TD.

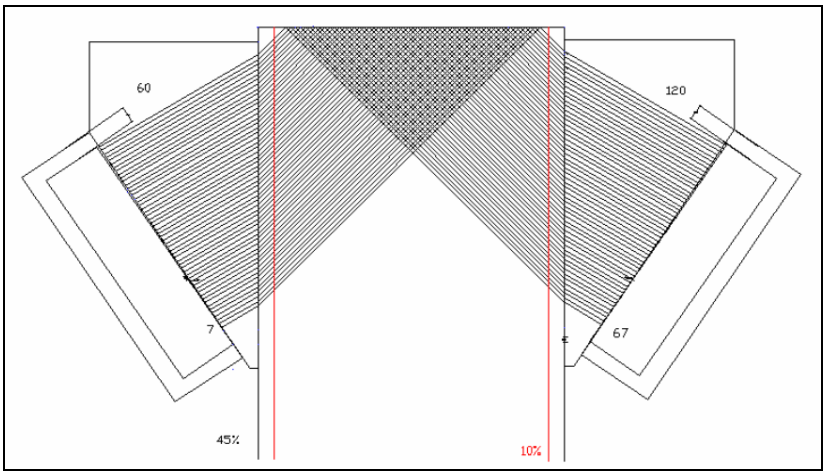

Figure 8. Electronic Scanning Configuration

Using this method and knowing the position of the flaw, probes can be statically placed along the side of the railhead, and an electronic scan of the flaw can be performed without moving the probes. A complete scan of the flaw takes only a few seconds.

Phase I of the program included a feasibility study to identify and compare current conventional ultrasonic rail inspection processes with ultrasonic PA approaches to inspect the railhead for TDs. Phase II of the program included identifying applicable inspection angles for use in the design, development, and implementation of an inspection transducer and wedge configuration that would provide rapid and reliable inspection and sizing of TDs located in the railhead. Phase II also included a Phase IIA that took the PA approach from the laboratory and implemented it into a field environment at FAST. Phase IIA used PAs to monitor characterized TDs in track during train and non-train operations.

3.1 Phase I: Feasibility of PA Ultrasonic Rail Inspection

The approach in Phase I of this research effort consisted of TTCI supplying several rail samples to RD Tech/Olympus NDT with and without internal TDs located in the head of the rail. During the feasibility study, two of the rail samples that were provided were primarily used for the evaluations. The defect in one of the samples was sized, using conventional contact ultrasonic sizing techniques at approximately 10 percent of the cross sectional head area (CSHA) of the rail. The defect in the other sample was sized at 45-percent CSHA. This feasibility effort was performed using a variety of different conventional ultrasonic inspection methods and an emerging PA ultrasonic inspection approach. With this method, the flaw can be located and sized.

3.1.1 Rail Flaw Evaluation Using Conventional Ultrasonic Probes

The conventional ultrasonic probes used to inspect the rail samples were 1/2-inch (12.7 mm)-diameter and 2.25-MHz transducers. By using the 2.2 MHz probe at the end of the rail that does not contain a TD, a reflected ultrasonic signal (back wall) created by the impedance mismatch at the opposite end of the rail can be seen (see Figure 9). Figures 10 and 11 show these procedures, representing a rail without a TD and a rail with a TD.

With the rail length and flaw location measurements, as determined by measuring the length of the rail and the location of the flaw, the velocity of sound, in the material, can be calculated. The velocity can be determined by monitoring the time of flight of the ultrasonic signal, which is the time it takes to reflect from a reflective surface (in this case the opposite rail end or the flaw). This can be calculated using the formula:

$$\text{Velocity (V)} = \text{distance (d)}/\text{time (t)}$$

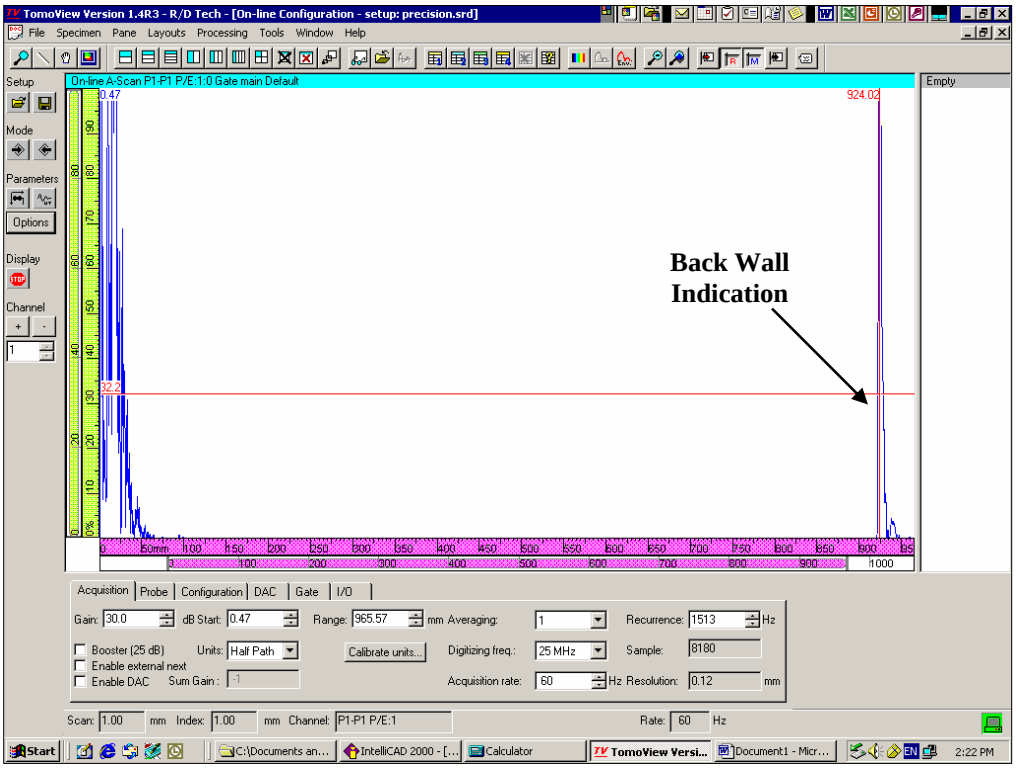

Figure 9. Rail with No Flaw Present Showing the Back Wall Reflection

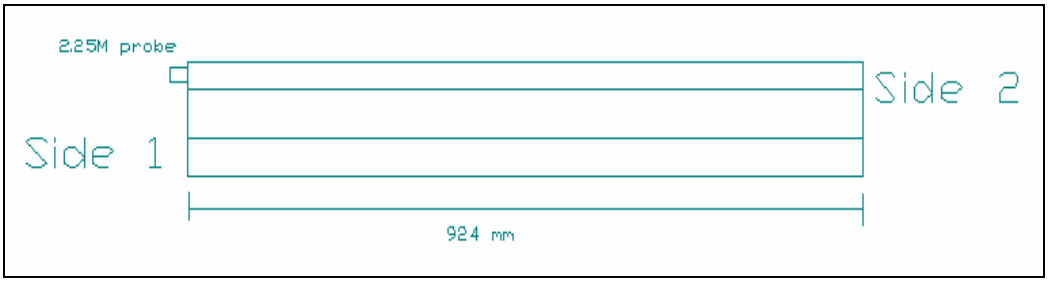

Figure 10. Side View of the Rail without a TD Showing the Conventional Probe Position

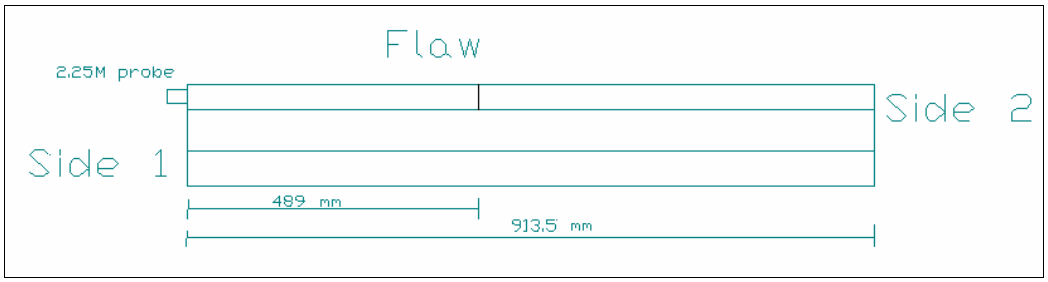

Figure 11. Side View of the Rail with a 10-percent TD Showing the Conventional Probe Position

3.1.1.1 Detecting a Flaw

Two 5 MHz probes, mounted on 33.7-degree wedges were placed on each side of the railhead and oriented face-to-face and used to size the flaw in the pitch catch mode of operation (Figure 12). The conventional approach was conducted in the same manner for both the rail containing the 10-percent TD and the rail with the 45-percent TD. Using this setup, the TD was detected, as Figure 13 shows, but the sensitivity to size the TD reliably is limited to the beam spread produced with this conventional approach.

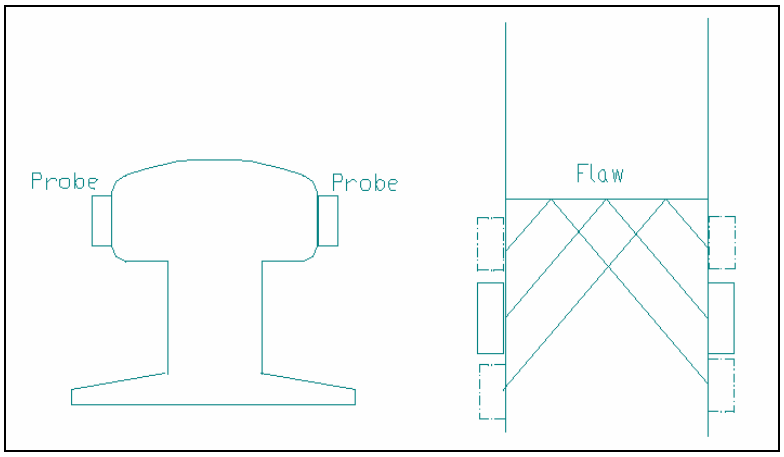

Figure 12. Manual Scan with Two 5 MHz Conventional Probes

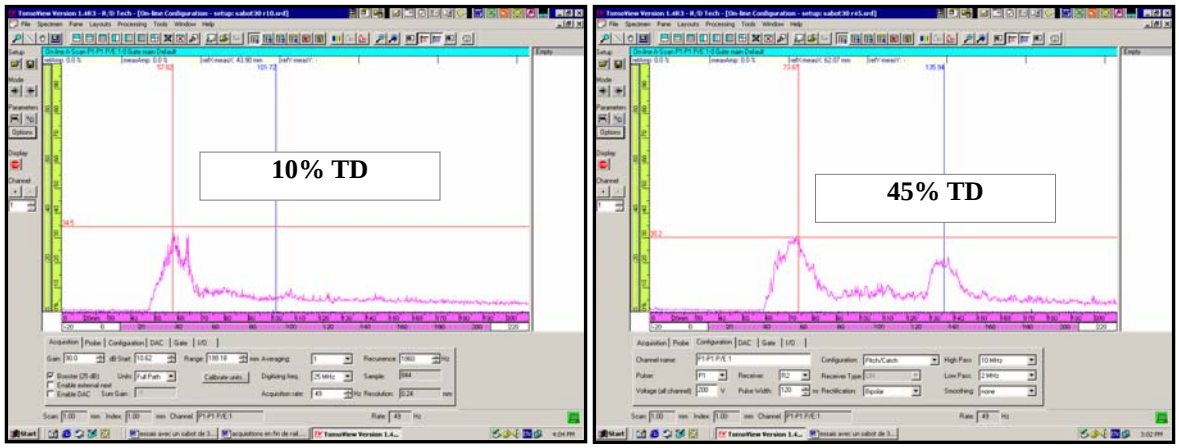

Figure 13. A-Scan Display Showing TDs During Inspection with Conventional Probes

The peak shown on the amplitude scan (A-scan) in Figure 14 is the signal coming from the TD that is located under a shell (horizontal separation). The shell is not detected in this setup because interrogation is being performed from the sides of the railhead, and the ultrasonic waves are oriented primarily parallel with and below the shell. In this case, this is advantageous because detection is focused on identifying TDs under shells or other forms of rail surface damage.

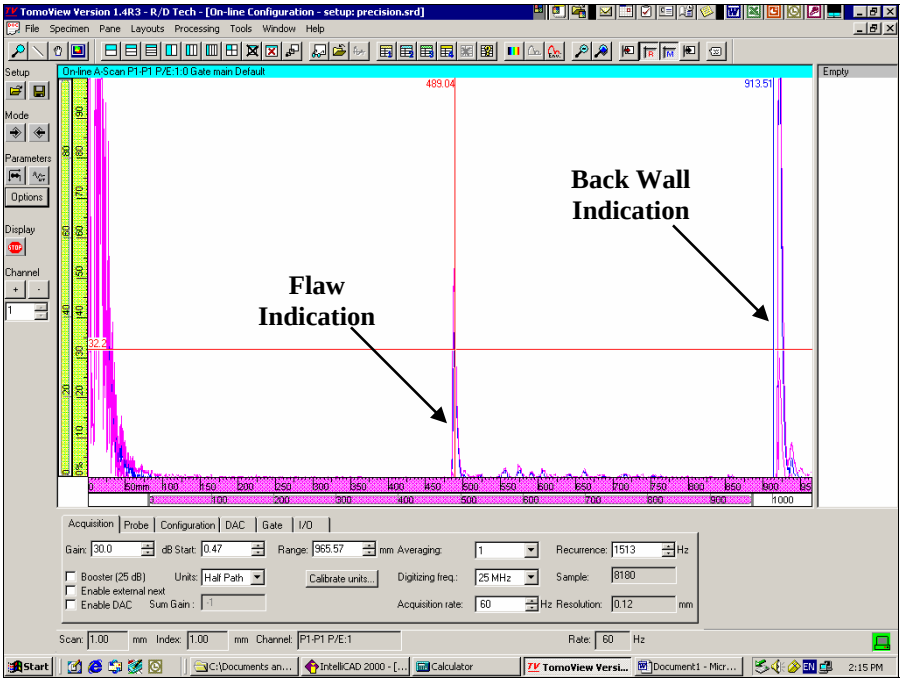

Figure 14. Location of the Flaw and Back Wall for the Rail with the 10-Percent TD

3.1.2 Rail Flaw Evaluation Using PA Probes

The inspection process using the PA probes again employed an approach that interrogates TDs from the side of the railhead. For calibration, the probes were placed in a position to detect the end of the rail, with the rail end representing a 100-percent CSHA TD. This allows for the determination of where the defect will appear in the sound path and the amplitude level necessary to detect the TD. Figure 15 shows an A-scan and plan view scan (C-scan) of the rail, with the rail end simulating a TD that extends all the way across the head of the rail.

Once calibration was complete, the same process was repeated for the rail samples containing the 10- and 45-percent TDs. Figure 16 shows the A- and C-scans of the rail containing the 10-percent TD. The C-scan shows that the transverse representation of the flaw across the railhead is much smaller than that represented by the rail end. The measured size of the TD, using the PA approach, shows the transverse length of the flaw to be 0.52 inch (13.2 mm). Given that the width of this railhead, from gage to field, is about 2.48 inches (63 mm), the width ratio between the flaw and railhead is then calculated to be approximately 21 percent. The 45-percent flaw, as Figure 17 shows, had a transverse length measured to be 1.51 inches (38.4 mm) with the railhead width being 3.07 inches (78 mm); the width ratio of this TD was determined to be 49 percent.

These sizes are representative of the width measurement of the flaw only and do not include the height of the flaw. This is why an ultrasonic sizing difference exists between the initial characterization of the TDs and the PA width sizing. The initial characterization of the flaws, using conventional probes, represents both the width and height measurements for the flaws.

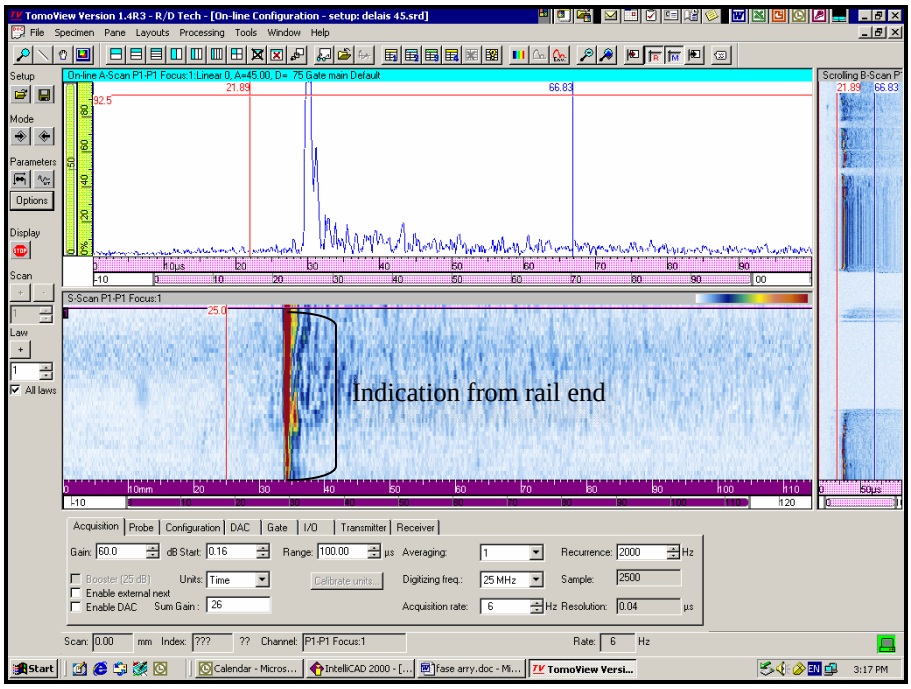

Figure 15. A-Scan (Top View) and C-Scan of the Rail End Representing a 100-Percent TD

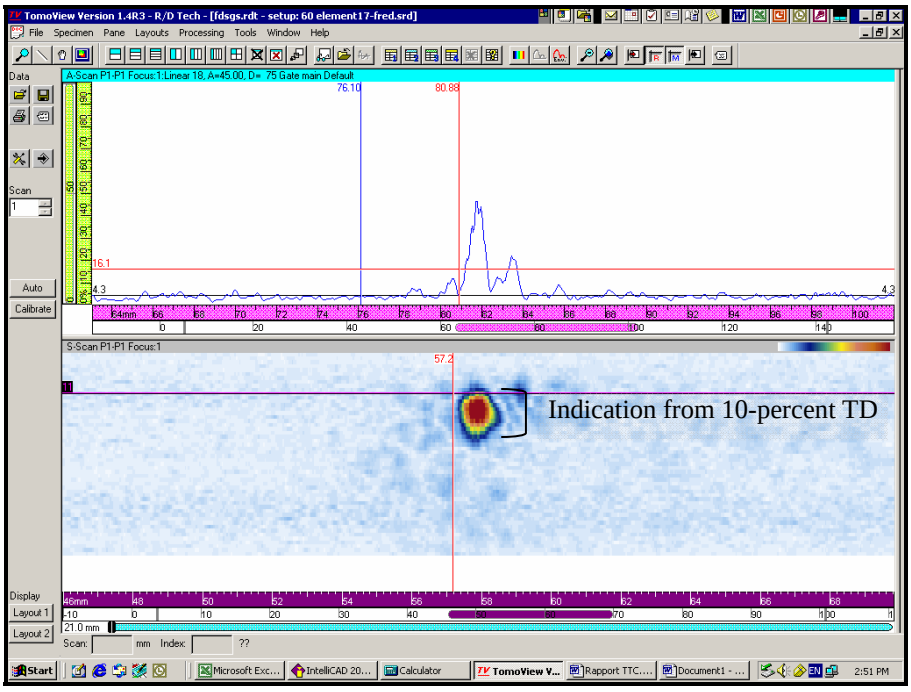

Figure 16. A- and C-Scans of the 10-Percent TD

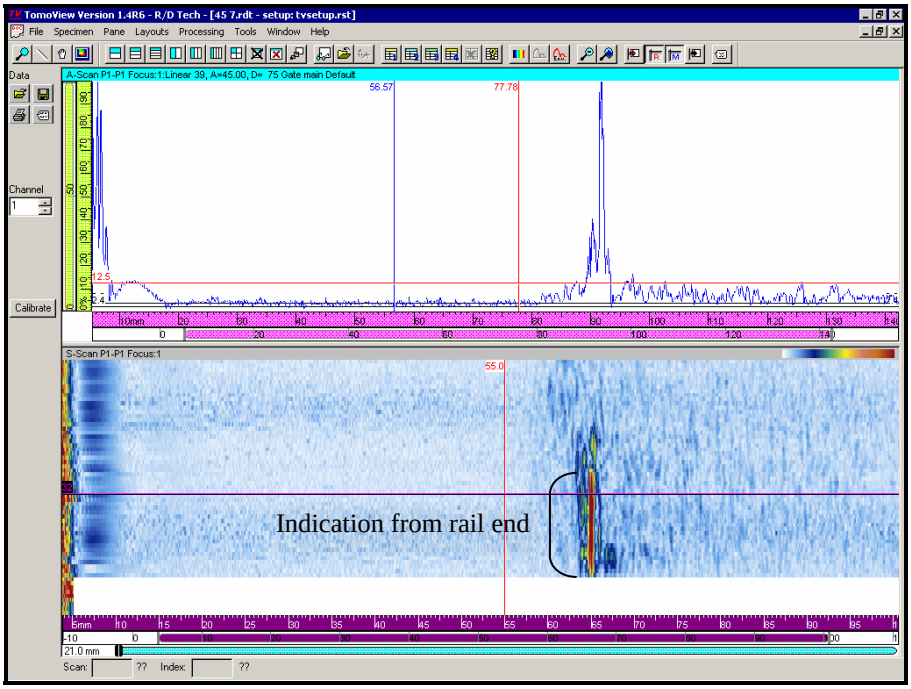

Figure 17. A- and C-Scans of the 45-Percent TD

3.1.3 Observations from Phase I Feasibility Study

Results of the feasibility study determined that a linear PA ultrasonic inspection approach has the capability to:

- Detect TDs and discriminate from a shell
- Determine the location of the TD in the rail
- Estimate the width of the TD

Amplitude alone does not provide an entirely accurate flaw size. This was demonstrated by the comparison between the amplitude of the 10- and 45-percent TDs evaluated. Using the same parameters, the amplitude of the 10-percent TD was greater than that of the 45-percent TD. Therefore, by basing the flaw size on amplitude alone, the smaller flaw in this case would be identified as a larger defect than the actual defect that was characterized as the larger of the two. The C-scan representation of the rail end and TDs shown in Figures 15, 16, and 17 provides a more reliable representation of flaw size with the width ratios of 100 percent (rail end), 21 percent (10-percent TD), and 49 percent (45-percent TD), respectively.

The positive results from Phase I provided the basis to continue research into the application of a PA approach for rail flaw inspection. In Phase II of this research, further evaluation of a PA approach to determine both width and height of TDs was performed.

3.2 Phase II: Sizing of TDs Using Ultrasonic PAs

Phase II of this research was performed to identify an inspection approach that uses the PA method to determine both the width and the height of TDs similar to that shown in Figure 18. The inspection was performed with PA technology and time of flight diffraction (TOFD) using conventional probes.

In Phase I of this research, an inspection approach was executed using two PA probes set up in the pitch-catch mode. The previous technique consisted of putting an angled PA probe at each side of the railhead before the defect area so that the pitch-catch mode of linear scanning could be applied. By counting the focal law number (individual beam pulses) of the receiver that catches the returned ultrasonic signals, the width of the TD was measured. This approach measures the width of the TD very efficiently and quite accurately. The configurations of the probes, however, require putting two PA probes at each side of the rail's head area. Thus, it is not suitable for in-service inspections of the railhead, where trains pass over the rails and their wheels pass through and damage any probe located on the gage side of the rail. Furthermore, the Phase I approach only accounts for width sizing and does not include sizing the defect's height. In Phase II, the sizing is done for the width and height of the defect, under the condition that the PA probes do not interfere with the wheels of the trains as it passes over the flaw area.

The same two rail samples used in Phase I, which contained known defects of 10-percent CSHA and 45-percent CSHA, were also used during Phase II of this research. The two sides, gage to field, of the railhead of the first specimen are nearly parallel, and the width is 2.97 inches (75.5 mm); those of the second specimen are not parallel, and the width is between 2.36 inches (60 mm) on one end of the sample and 2.76 inches (70 mm) on the other end. The following

sections will refer to the specimens with the 45-percent CSHA TD as Sample A and the other (10-percent TD) as Sample B.

The PA probe models used in this phase of the research were 5L60E60-10, which is a 5 MHz, 60 element probe, with a length of 2.36 inches (60 mm) and an element width of 0.39 inch (10 mm) and 7.5L60E60-10, which is a 7.5 MHz with the same element, length, and width setup as the 5 MHz probe. The wedges are made of a rexolite phenolic with wedge angles of 40 and 33.7 degrees, respectively. Inspections are performed with angled shear waves. The scans are linear or sectorial (azimuthal or angular scans) in the horizontal plane. The inspections were performed in a water tank to ensure continuous acoustic coupling between the wedge and the railhead.

3.2.1 Sectorial Scan (S-Scan)

The sectorial scan (S-Scan), also called azimuthal or angular scan, uses a beam steering process to interrogate a material. Inspection is carried out as the beam is steered or moved through a sweep range setup for a specific focal depth(s), using the same elements (Figure 18). This configuration can provide a large visual scope inside the rail.

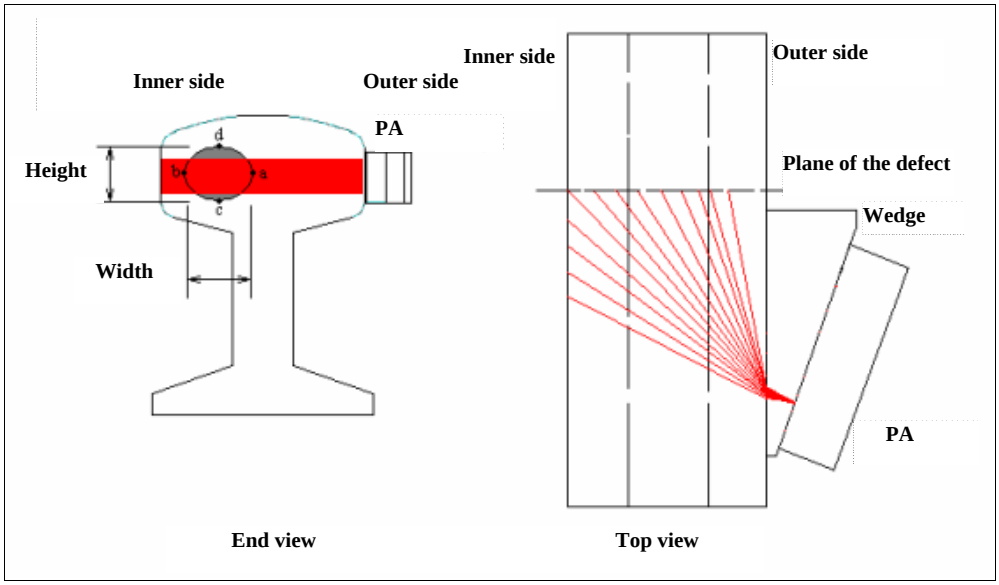

Figure 18. Sectorial Scan

3.2.2 Linear Scan

Linear scanning, as identified in Phase I, is performed by scanning in a line along the railhead while the array performs an electronic scan of the material. The same configuration as in Figure 18 is used to determine the defect's width by counting the focal law number that detects the back-reflected echo from the defect. This number is directly related to the defect width. The defect width is defined by the distances *a*-*b*.

3.2.3 Width Sizing with Azimuthal Scan

With the configuration shown in Figure 18, the azimuthal scan was performed to determine the width of the flaws. Figures 19 and 20, respectively, show the results of the two rail samples. The strongest signals are the corner reflection near point b (see the sketch under each B-scan). The most useful signals related directly to the defect width are the diffractions from point *a* and *b*. The reflections from the defect surface are not found in the figures. For Sample A (Figure 19), the defect begins in the width direction at 1.65 inches (42 mm) and stops at 2.80 inches (71 mm), making the width of the defect 1.14 inches (29 mm) (i.e., 38 percent of this rail width). For Sample B (Figure 20), the defect begins at 2.20 inches (56 mm) and stops at 2.68 inches (68 mm) for a difference of 0.47 inch (12 mm), divided by the maximum rail width of 2.76 inches (70 mm), making the width ratio 17 percent between the railhead width and the width of the TD for Sample B.

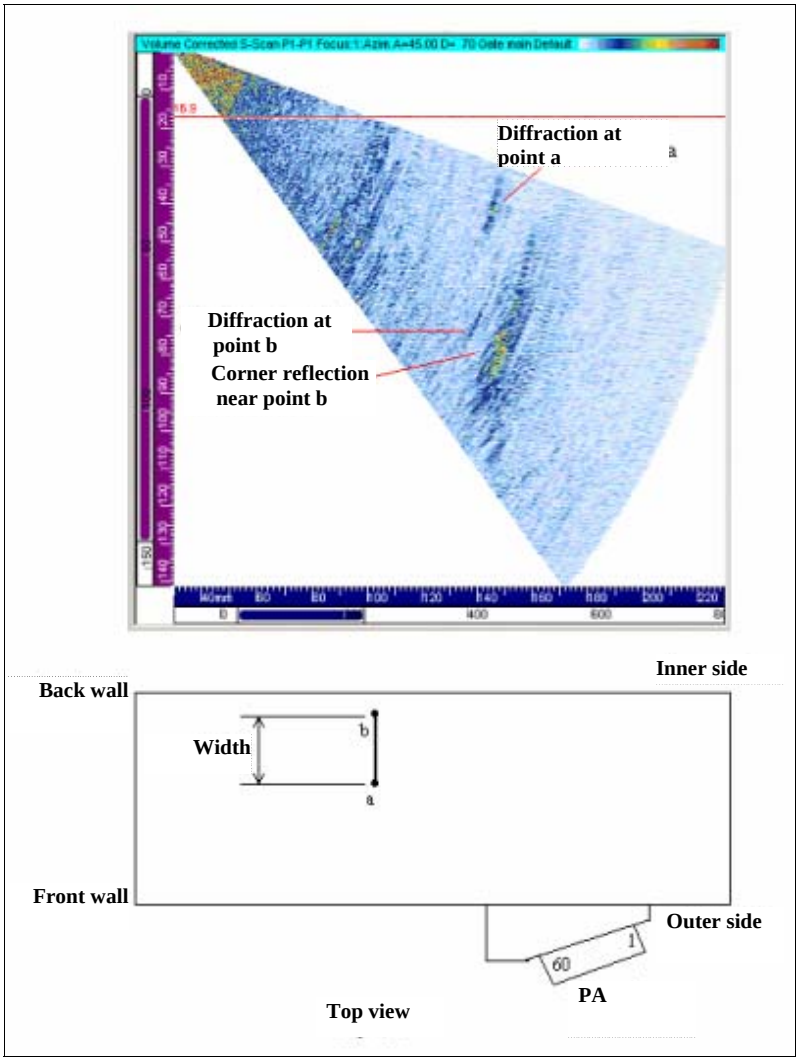

Figure 19. Azimuthal Scan on Rail Sample A, Measurement Conditions: Probe Frequency: 7.5 MHz, Scanning Angle: 40 to 75 Degrees, PA Aperture: 32 Elements, Wedge Angle: 33.7 Degrees

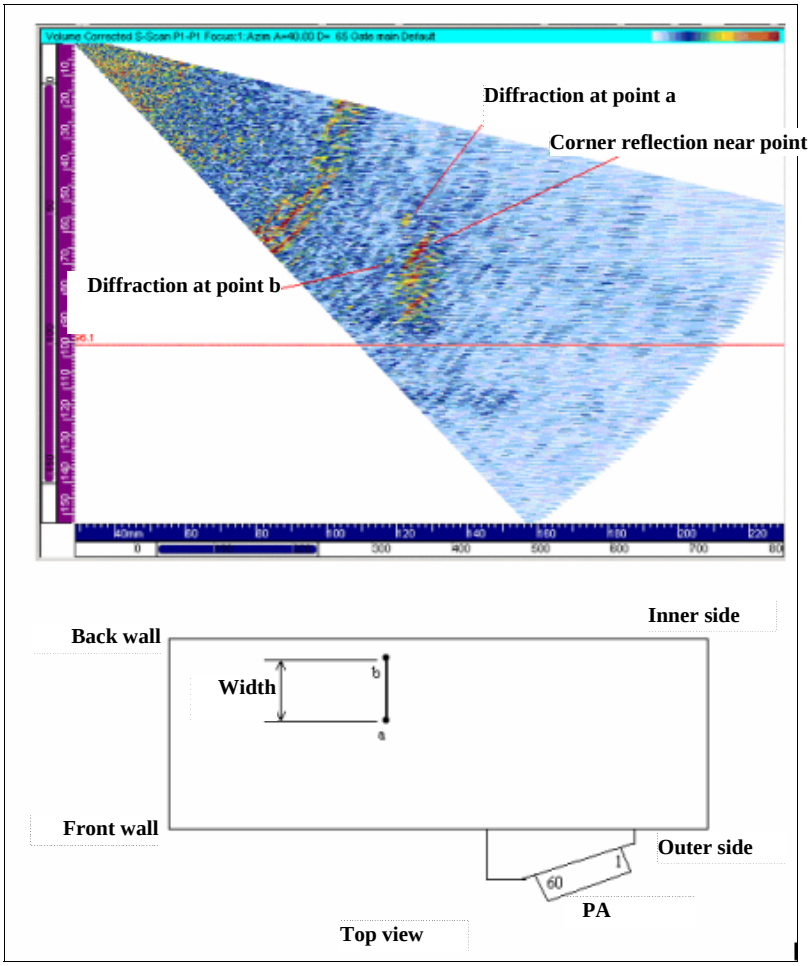

Figure 20. Azimuthal Scan on Rail Sample B, Measurement Conditions: Probe Frequency: 7.5 MHz, Scanning Angle: 40 to 75 Degrees, PA Aperture: 32 Elements, Wedge Angle: 40 Degrees

Similar results were produced in Phase I using the linear scanning approach (Figure 18). That approach showed the width ratio between the TD and railhead to be approximately 49 percent for Sample A and 21 percent for Sample B. This result reflects the need for consistency in calibration but is close enough to provide a determination of an approximate size of the TD. The reflection from the defect surface could not be seen with the linear approach, so the idea of counting the focal law numbers to detect and size the defect was not achievable. The limitation of the linear scan is the narrow visual scope of the PA; the PA cannot consistently see all the indications together. A smaller probe that provides more coverage can be used with the sectorial scan in this application.

3.2.4 Height Sizing

3.2.4.1 PA Approach

Figure 21 shows the configuration for height sizing using the PA approach. The same PA probe as identified previously was used. The wedge angles are 31 and 43 degrees, respectively. These wedge angles ensure that diffracted shear wave angles of 45 and 74 degrees are generated into the rail steel. The scan is linear and in the vertical direction. The intent of this configuration is to try to determine the TD's height by counting the focal law number that detects the back-reflected echo from the TD. This number is directly related to the defect's height.

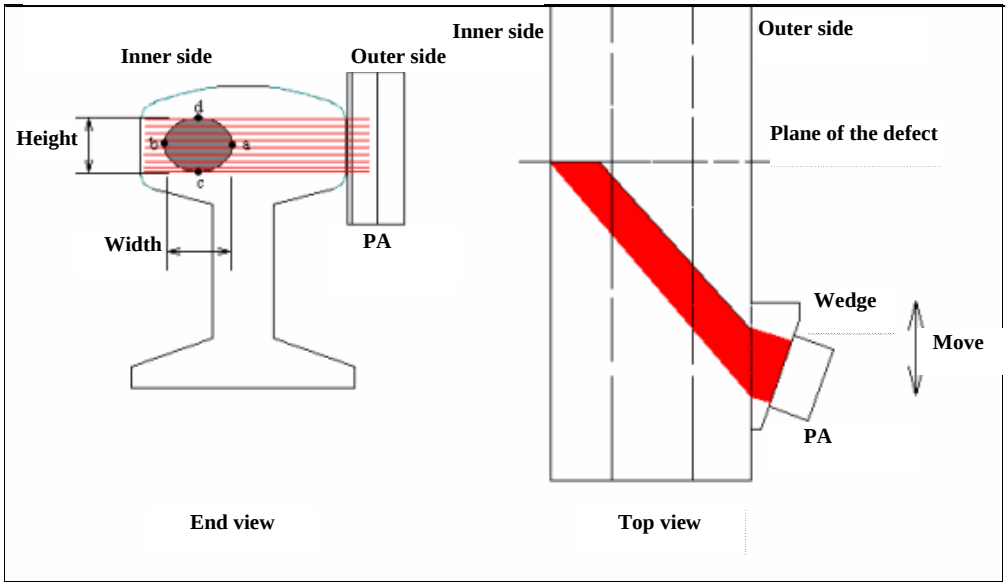

Figure 21. Vertical Scan Using a Linear PA Approach with the Defect Height Defined by the Distance *c-d*

Figure 22 (Sample A, wedge angle 31 degrees and 5 MHz probe) shows the corner reflection near the edge (point *b*) of the defect, and Figure 23 (Sample A, wedge angle 43 degrees and 7.5 MHz probe) shows both the corner reflection near point *b* and the diffraction near point *a*. Because the gage and field sides of the railhead are parallel to each other, the defect's height that is creating the ultrasonic reflections can be estimated by counting the focal law number. From these figures, the height related to the corner reflection is roughly 0.63 inch (16 mm), and the height related to the diffraction near point *a* is roughly 0.75 inch (19 mm). A more accurate height sizing can be accomplished with a more detailed calibration procedure. Although the exact positions of the heights cannot be known, these heights can be considered as a first approximation of the height from point *c* to point *d* (see Figures 22 and 23).

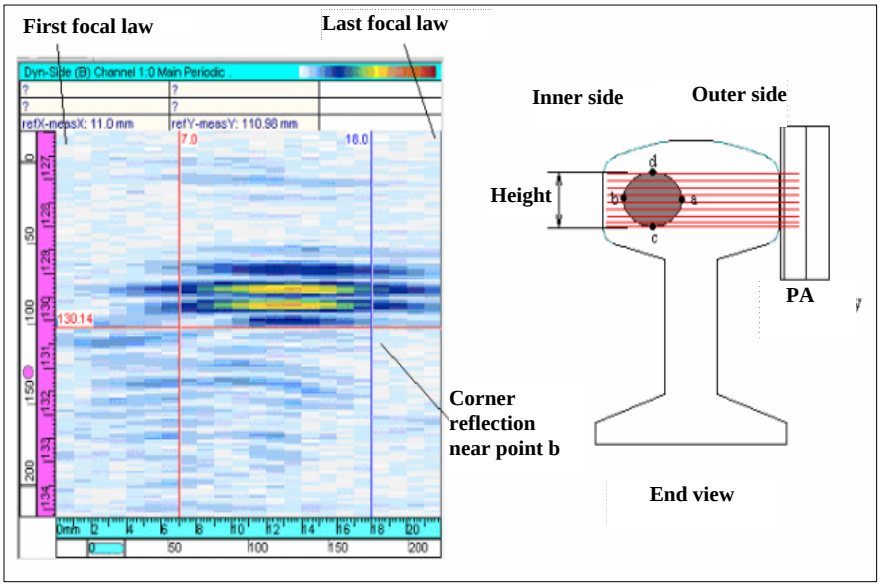

Figure 22. Height Sizing Using PA Showing the Corner Reflection Near Point b, Measurement Conditions: Sample A, Wedge: 31 Degrees, Inspection Angle: 45 Degrees, Probe Frequency: 5 MHz

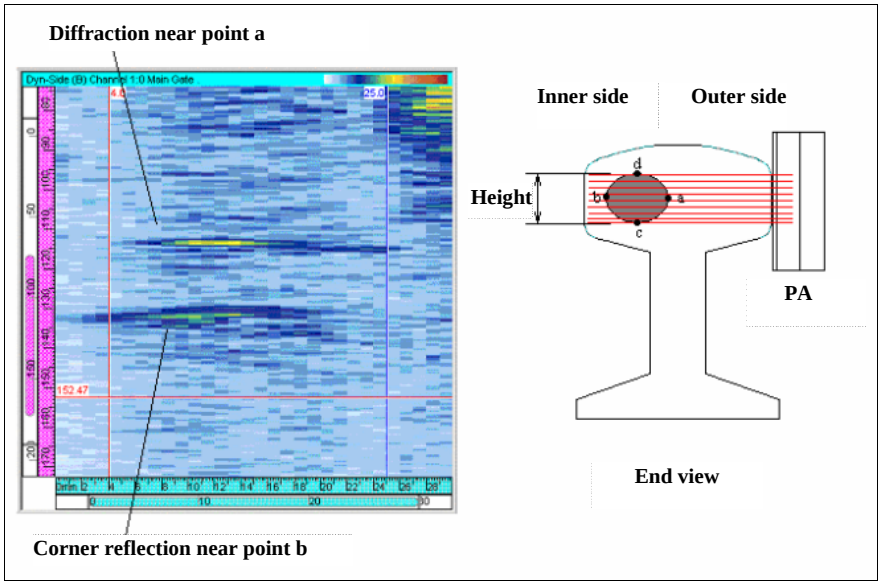

Figure 23. Height Sizing Using PA Showing Both the Corner Reflection Near Point b and the Diffraction Near Point a, Measurement Conditions: Wedge Angle: 43 Degrees, Inspection Angle: 74 Degrees, Probe Frequency: 7.5 MHz

Figure 24 (Sample B, wedge angle 31 degrees and 5 MHz probe) shows the corner reflection near the edge (point b) of the defect, and Figure 25 (Sample B, wedge angle 43 degrees and 7.5 MHz probe) shows the corner reflection near point *b* and the diffraction near point *a*. Because the gage and field sides of the railhead are parallel to each other (see Figures 24 and 25), the defect's height that is involved in the reflection cannot be estimated by counting the focal law number. From Figure 25, the height related to the diffraction near point *a* is roughly 0.20 inch (5 mm).

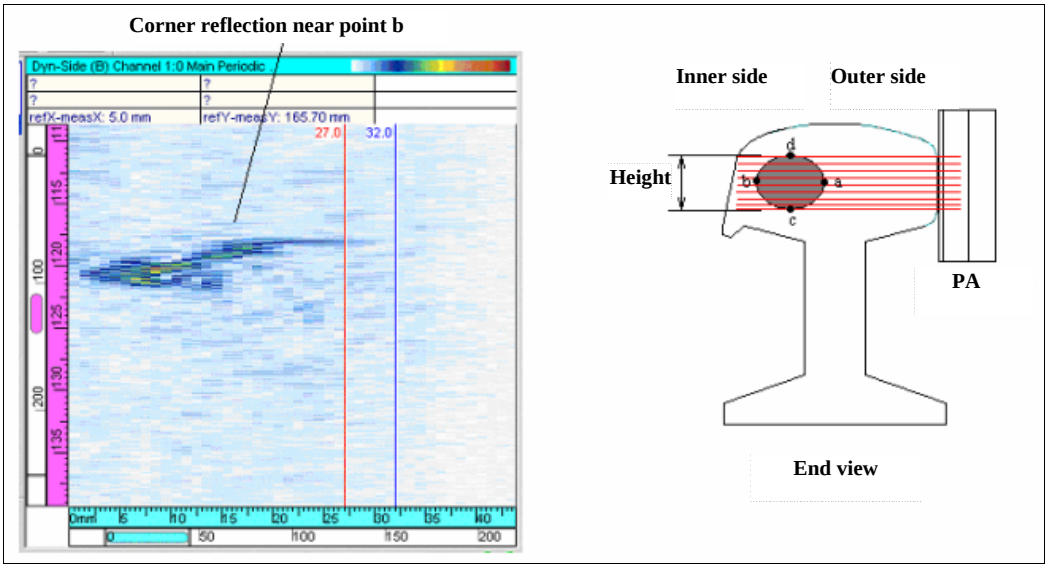

Figure 24. Height Sizing Using PA: Corner Reflection Near Point b, Measurement Conditions: Sample B, Wedge Angle: 31 Degrees, Inspection Angle: 45 Degrees, Probe Frequency: 5 MHz

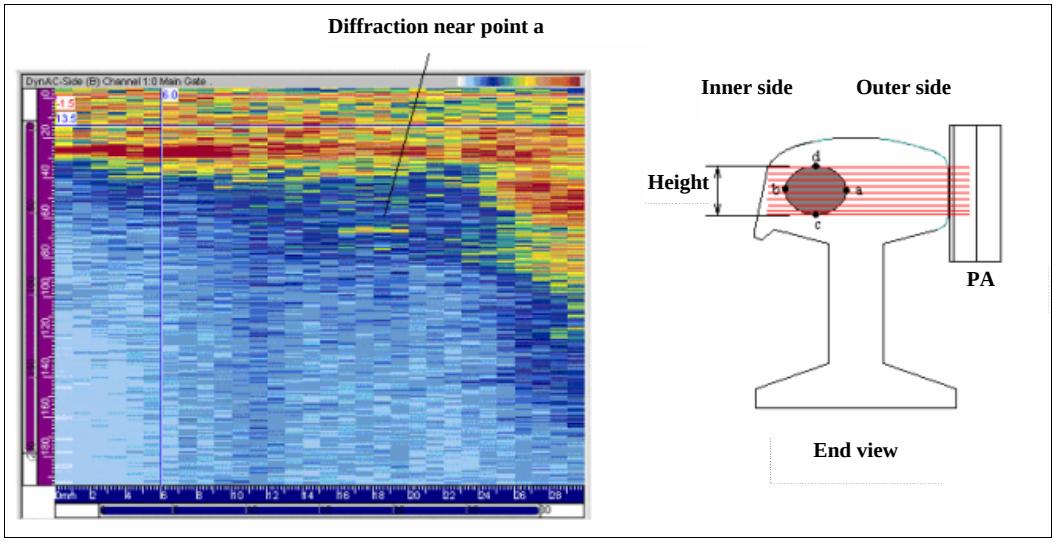

Figure 25. Height Sizing Using PA Diffraction Near Point a, Measurement Conditions: Sample B, Wedge Angle: 43 Degrees, Inspection Angle: 45 Degrees, Probe Frequency: 7.5 MHz

3.2.4.2 TOFD Approach Using Two Conventional Probes

The TOFD method was also considered (see Figure 26) for sizing the TD. In this setup, two conventional probes with frequencies of 5 MHz were used. The wedge angle used was 60 degrees (optimized). According to the positions of the probes shown in Figure 26, the detected height is an approximation of the distance *c-d*.

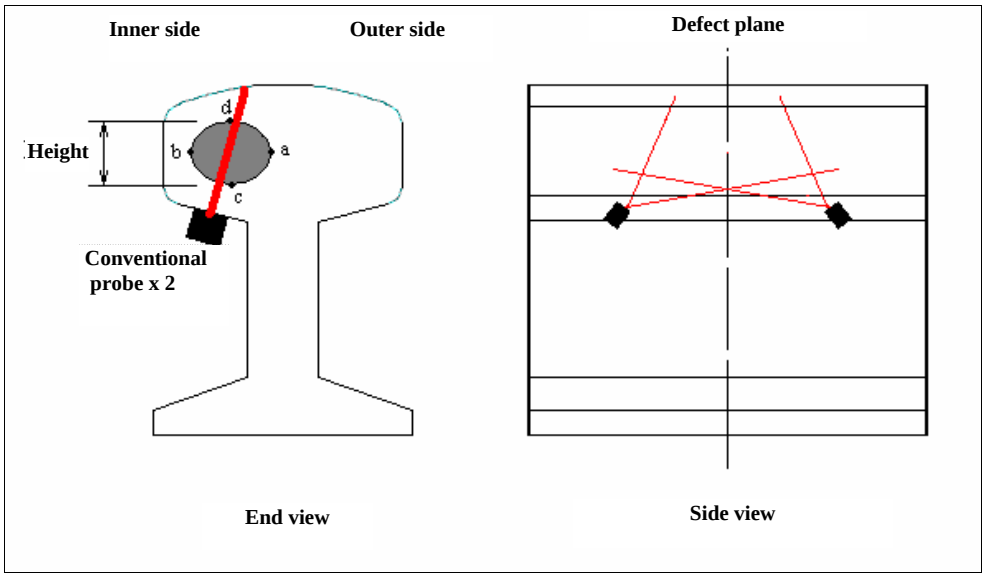

Figure 26. TOFD Configuration on Rail

The TOFD method is classic. It uses two wedged conventional probes face-to-face to generate angled longitudinal beams in the material. For the configuration shown in Figure 26, normally the first waves to arrive in the A-scan are the lateral waves, then the diffracted waves from the near edge of the defect (near point *c*), and finally the diffracted waves from the far edge of the defect (near point *d*). Because the back wall is not parallel to the beam-entering surface, a reflection may not be detected.

Figures 27 to 30 show the resulting scans. For comparison, measurements were performed in the defect area and the defect free area, respectively. Figures 27 and 28 show the results of Sample A, and Figures 29 and 30 show the results of Sample B.

By comparing Figure 27 with Figure 28 (for Sample A), a difference is shown in the radio frequency and B-scan presentations. In the defect area, the lateral wave is highly attenuated, signifying the defect edge is very near the beam-entering surface. In Figure 27, after the trace of the lateral wave, another wave appears, representing the diffraction from the far edge of the defect (point *d*).

For Sample B, Figure 29 (defect area) shows the lateral waves and the two typical crack tip diffraction waves with opposite polarization. As a comparison, the lateral waves appear in Figure 30 but without crack tip diffractions. In the experiment, the crack tip diffractions are not always easy to see: the signal depends on critical position or orientation of the probes (the

contact surface is not ideal). This limitation will have to be addressed for in-service dynamic inspection, where the vibrations over track could be very strong.

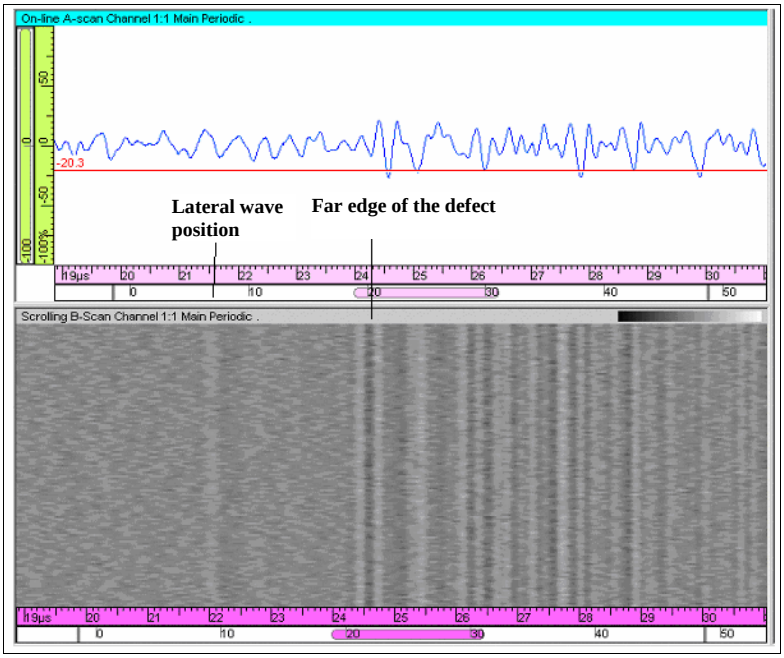

Figure 27. TOFD for Height Sizing in the Defect Area for Sample A

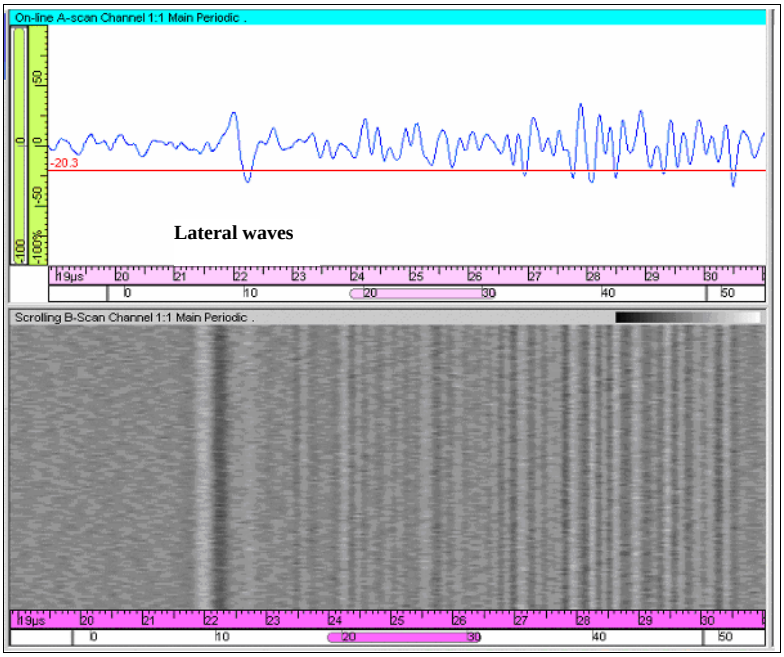

Figure 28. TOFD Inspection for Sample A in a Defect Free Area

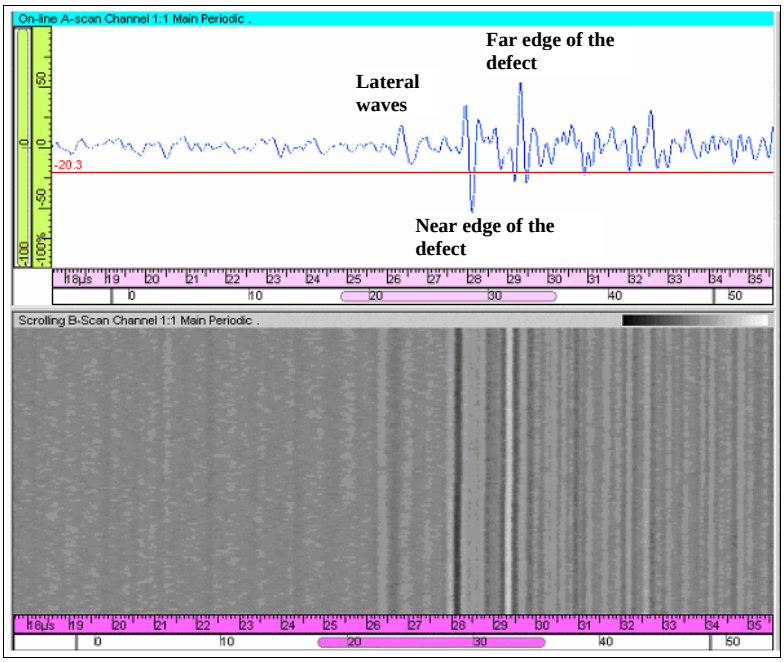

Figure 29. TOFD for Height Sizing in the Defect Area for Sample B

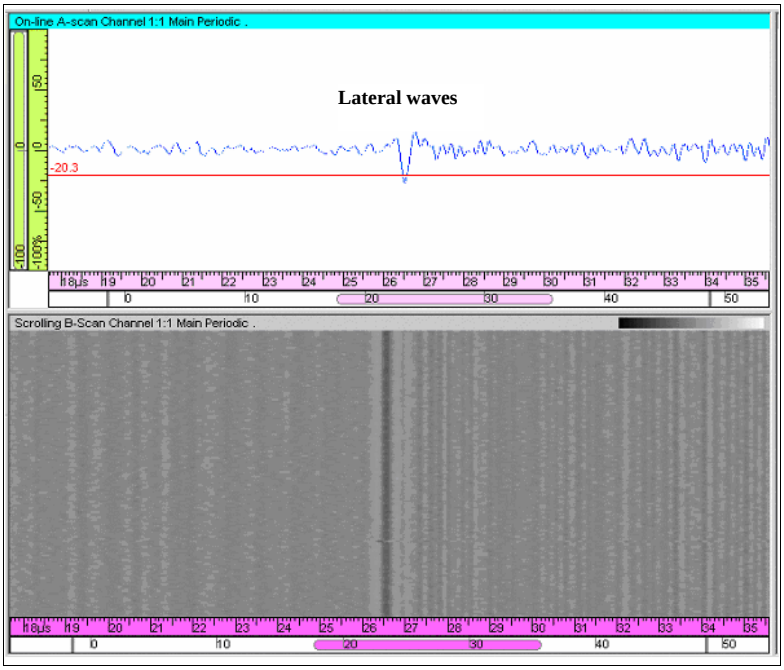

Figure 30. TOFD Inspection for Sample B in a Defect Free Area

The defect height can be estimated using the conventional height measurement technique of the TOFD (here there is a wedge delay of 6 μm to remove). The calculated results are as follows (suppose longitudinal wave speed is 5.9 mm/μs):

Sample A:

Distance between two probes = 3.67 inches (93.2 mm)
Sound path to reach Upper Tip = 4.25 inches (108 mm)

As a result, the depth of the defect is 1.06 inches (27 mm). Because the near edge of the defect almost reaches the surface, the defect height is approximately 1.06 inches (27 mm).

Sample B:

Distance between two probes = 4.65 inches (118 mm)
Sound path to reach Upper Tip = 5.02 inches (127.4 mm)
Sound path to reach Lower Tip = 5.32 inches (135.2 mm)

As a result, the height of the defect is 0.35 inch (8.9 mm).

Both calculated heights are greater than the heights estimated by the PA height sizing. PA height for Sample A was 0.75 inch (19.05 mm) compared to the TOFD height of 1.06 inches (27 mm). PA height for Sample B was 0.20 inch (5.08 mm) compared to the TOFD height of 0.35 inch (8.9 mm). This deviation in height can again be attributed to calibration. As research in this area continues, a more detailed calibration procedure will be developed to assist in increasing the accuracy and repeatability of sizing. Although a variance in the height size is determined by the PA and conventional (TOFD) approaches, they are both accurate enough to determine a rough estimate in the size of the TD when considering whether the flaw is small (0 to 10 percent CSHA), medium (11 to 30 percent CSHA), or large (greater than 30 percent CSHA).

3.2.5 Observations from Phase II: Sizing of TDs Using Ultrasonic PAs

Both PA and TOFD techniques have been studied for sizing of TDs. The possibility of sizing both the width and the height of TDs has been demonstrated. The advantage of using the PA approach, for width sizing, can be found in the ease for which localizing or identifying diffracted waves from the defect can be done without moving the probe. Information on the width is clear, and the sizing is quite reliable. A possible problem in practice may be the difficulty in the determination of the diffraction from point *b*.

Height sizing using the PA approach can be considered as a first estimation of the true defect height. Height sizing using the reflection mode could not be used because the reflection signal was weak even at a very high angle, and the time of flight was very near the corner reflection and the edge diffraction at point *a*. Height sizing estimation may also be performed using conventional probes as a low-cost impact. The TOFD technique can be useful for the height sizing, while a robust solution should be found for online inspection.

A calibration procedure must be established to ensure the accuracy of both width and height sizing. Compared with the sizing method reported in Reference 2 (use of two PA probes fixed at each side of the railhead in pitch-catch mode), the present work is more convenient for revenue

service monitoring. To improve the beam properties, the use of Dynamic Depth Focusing (DDF) is suggested. DDF will keep the beam narrow through the thickness of the material; it should reduce the noise level and improve the detection level of crack tip diffraction coming from the flaw. The important thing is to analyze and understand the signals. PA gives a better view inside the rail, but the operation will still need to understand how to interpret the different echoes generated during the inspection. The interpretation may also be analyzed and addressed with software identification or development between the different echoes.

3.3 Phase IIA: Sizing of TDs at FAST Using Ultrasonic PAs

Phase IIA took the PA approach evaluated in the laboratory and implemented it into a field environment at FAST. Phase IIA used PAs to monitor characterized TDs in track during train and non-train operations. The PA ultrasonic approach being developed and evaluated uses a series of focal laws and custom setup files to provide detailed images of transverse cracks in a railhead. A-, B-, C-, and D-scans of the flaw are processed together as sectorial or S-scans to provide detailed images of the TD. Figures 31 and 32 show the setup of the flaw monitoring process used to perform width and height sizing from the rail's field side.

Accuracy of flaw sizing can be influenced by the rail's longitudinal stress state and by defect orientation. Under this PA effort, research is being conducted to determine the sensitivity required for reliable and repeatable detection of railhead cracks under varying levels of longitudinal stress conditions and flaw orientations. During this effort, a PA transducer was positioned at the field side of a railhead sample containing a previously characterized TD. By using a raster scanning approach, the TD is continuously monitored ultrasonically, and scans are stored periodically to document the flaw size.

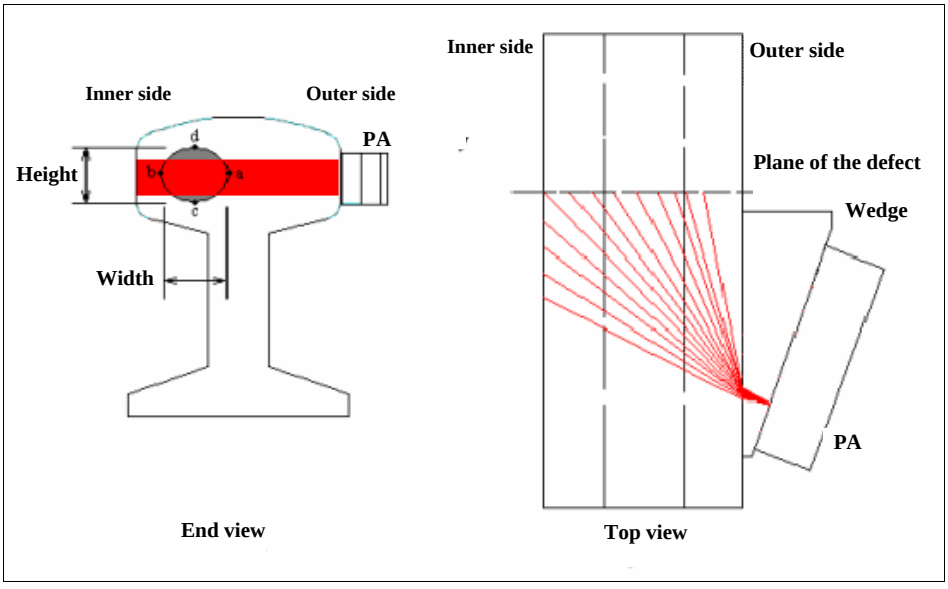

Figure 31. PA Railhead Width Sizing from the Field Side of the Rail

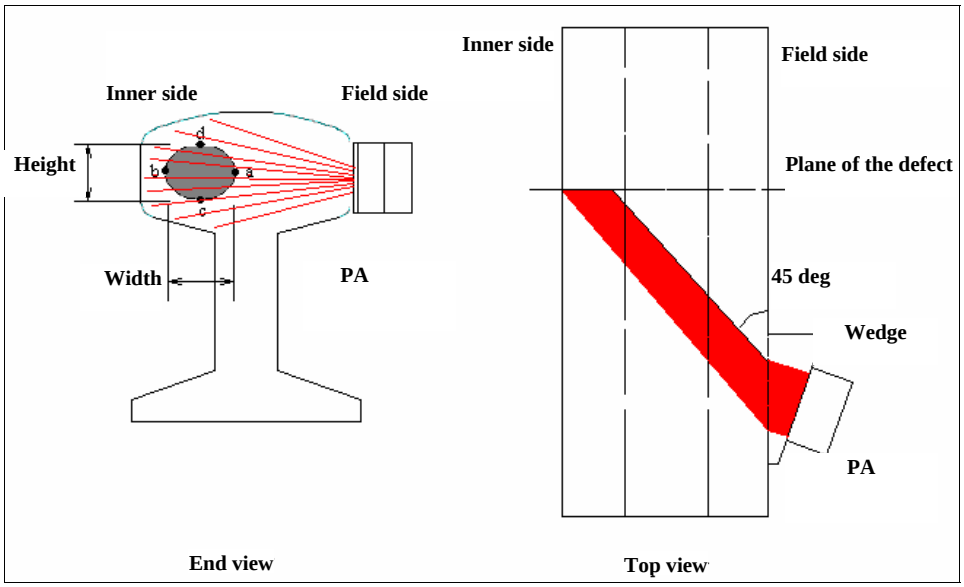

Figure 32. PA Railhead Height Sizing from the Field Side of the Rail

3.3.1 PA Setup at FAST

During the fall of 2005, under FRA sponsorship, TTCI set up a PA Omni-scan system to monitor a TD in track at FAST during train operations (Figure 33 and 34). The PA approach was used to document and observe variations and effects on flaw growth under heavy axle load (HAL) traffic. Flaw size comparisons were made during train operations and non-train operations over the flaw area. This effort was conducted to determine the repeatability and accuracy of the PA system.

Figure 33. (Top) PA System Setup at FAST; (Bottom) Field Side Location of PA Transducer on Railhead

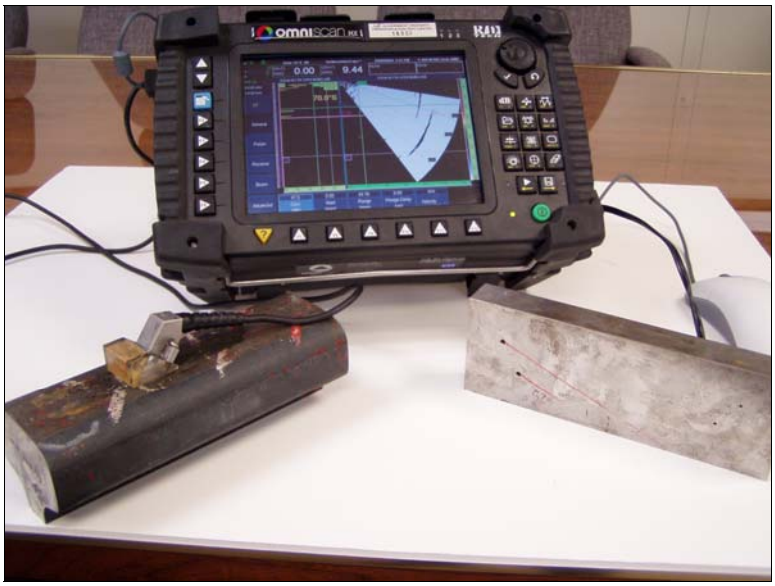

Figure 34. Omni-Scan PA System Used at FAST

3.3.2 Results from PA Monitoring at FAST

A PA in track evaluation was initiated at FAST in September 2005. The first rail sample used in the evaluation was identified as PA Sample 1 (PAS1). PAS1 consisted of a standard 136-pound/yard rail that contained a TD that was ultrasonically sized to be 12 percent of the rail's CSHA. The TD's orientation was primarily perpendicular to the top of the railhead and aligned across the head from gage to field.

Positioning the PA probe, on the field side of the railhead for width sizing, requires the monitoring of a virtual vertical line that can be drawn between one end of the crack and the other. The vertical line is displayed on the S-scan and starts on the left side of the corner trap, as Figures 35 and 36 show. This virtual line can be seen as the probe is moved along the side of the railhead. The line represents the defect surface. To optimize the defect location, the probe is moved back and forth with a little skew (angling of the probe), until the longest vertical line is determined. Points *a* and *b* display the diffracted signals from the crack ends (Figure 35). This scan shows the detected location of the TD, and Figure 36 shows the scan of the flaw after optimization of the PA signals.

Once the signals associated with the defect were optimized, the probe location was then fixed on the railhead side. Sometimes point *b* was not easy to determine because the TD is very near to the gage side of the railhead. In this case, an approximation for point *b* (back wall) was made. The defect width was measured directly using the cursors. The cursors are positioned across the center of the crack tip indications. Because the signal may be noisy, due to material and length of probe cable used (approximately 75 feet), some patience was required to find the most representative scan of the width, especially when the defect has a contoured surface, (growth rings) as was the case with the TD in PAS1. When unsure of the flaw signal location, operators can perform sizing by measuring both sides of the defect.

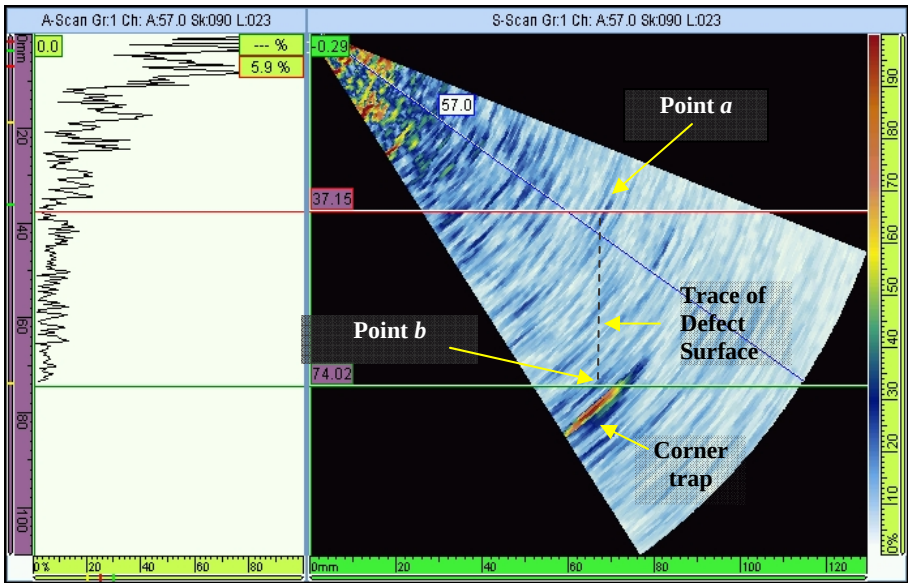

Figure 35. PA Scan of PAS1 Showing the Flaw Width Between Points a and b

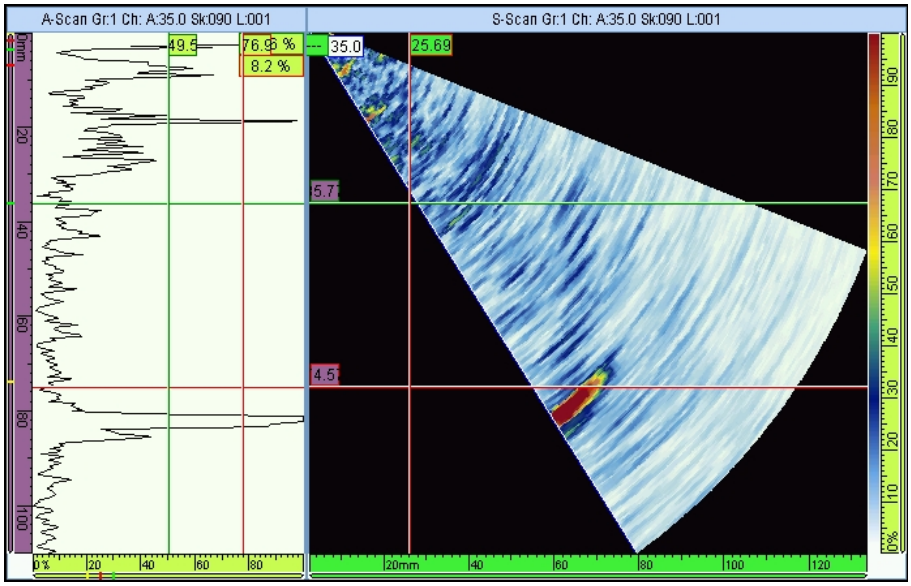

Figure 36. PA Scan of PAS1 Showing the Flaw Width After Optimization of Scan

The PA scans shown in Figures 35 and 36 show the width of PAS1. Using the horizontal cursors, Figure 35 shows the isolated flaw between the markers located at 1.46 inches (37.15 mm) and 2.91 inches (74.02 mm). The difference between the markers represents the TD width, which, in this case, is 1.45 inches (36.83 mm). Figure 36 shows the flaw after optimizing the scan. The markers show the actual PA sized width of the TD to be 1.2 inches (30.48 mm).

Generally the height sizing was found to be less accurate than the width sizing because the PA cannot efficiently determine the height using the focal law approach due to the geometry of the railhead. To optimize the signal from the TD, the corner trap signal is identified; the probe is

then moved towards the defect, thus allowing the ultrasonic beams to reflect off the defect area. The time of flight to the defect area is always before the corner trap. The corner trap is not always easy to identify because the back wall of the rail may not be vertical, so some skewing of the probe had to be performed to identify the corner trap. The flaw height was then determined by using the diffracted signals from the defect area, not the corner trap.

The diffraction from the defect area represents a reflector or target in the area but may not represent the height measured from point *c* to point *d* (Figure 37). To get the measurement from *c* to *d*, operators must move the probe over the scan area to optimize the indications received from the crack tips, making the scan zone as wide as possible. The rail surface (rail top, rail back wall) may also appear as an indication: operators can simply apply a wet finger to the rail surface, which will reduce (dampen) the response of the signal at the surface, allowing differentiation between the crack tip and rail surface signals. Operators may also scan from either side of the TD to determine flaw height because scanning from either side usually produces the same sizing result. Because the indication zone depends on the gain (with more gain, the zone seems larger due to amplification of the electronic signals that represent the returned ultrasonic signals), operators may use a -6 db amplitude drop method to determine the zone limits.

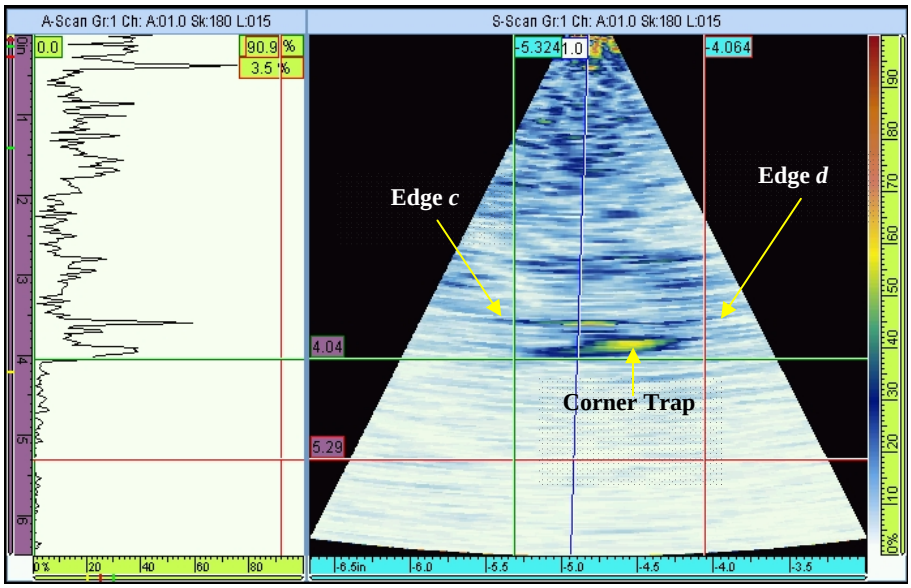

Figure 37. Height Sizing Probe Setup for PAS1

Using this approach for height sizing, the height of the TD in PAS1, Figure 37, can be measured at 1.26 inches (32 mm). The height and width of the TD shown in Figures 36 and 37 will now allow for the determination of the ultrasonic size estimation of the flaw. The flaw area is determined by using the height a and width b in the formula for the area of an ellipse as follows:

Flaw Area = πab

Where a is the flaw width divided by 2

and b is the flaw height divided by 2

Example:

a = flaw width/2 = 1.2/2 = 0.60 inch (15.24 mm)

b = flaw height/2 = 1.26/2 = 0.63 inch (16 mm)

Flaw Area = $\pi(0.60 \times 0.63) = 1.17$ inch^2 (9.6 mm^2)

The size of the flaw, when reported as percent CSHA, is dependent on the cross-sectional area of the railhead. This means that for the same size of TD, the percent CSHA will be greater for a smaller size or worn rail section than for a larger size or new rail section. The TD measured in PAS1 and presented in Figures 36 and 37 would therefore represent a larger percentage of CSHA in a 115-pound/yard rail section than in a 136-pound/yard rail section. AREMA's *Manual of Recommended Practices* for the manufacturing of rail shows the railhead area for a 115-pound/yard rail to be 3.92 inch^2 (99.97 mm^2) and the area for a 136-pound/yard railhead to be 4.82 inch^2 (122.43 mm^2) (4). The size of this flaw in the 115- and 136-pound/yard rail sections would then be:

Example (115 pound/yard): TD% = (Flaw Area / Rail Head Area) * 100

= (1.17 in.^{2} / 3.92 in.^{2}) * 100

= 0.298 * 100

= 29.8%

Example (136 pound/yard): TD% = (Flaw Area / Rail Head Area) * 100

= (1.17 in.^{2} / 4.82 in.^{2}) * 100

= 0.243 * 100

= 24.3%

Because the size of the rail section being evaluated (PAS1) was 136 pound/yard, the percent CSHA for the TD represented in Figures 36 and 37 was approximately 24 percent. The defect in the PAS1 sample had an ultrasonically measured size of 12-percent CSHA when it was installed at FAST. The 24-percent size was measured after the flaw had undergone approximately 6

million gross tons (MGT) of 315,000 pound/car HAL traffic. Table 1 shows the flaw size after every 2 MGT of accumulated HAL traffic at FAST. The table also shows the minimum, maximum, and daily change in rail temperature at 2 MGT intervals. The graph in Figure 38 represents the growth of the TD in PAS1 as monitored in track at FAST. The data shows that the TD grew from 12- to 42-percent CSHA after approximately 22 MGT of HAL traffic at FAST.

Table 1. PAS1 Ultrasonic Flaw Sizes in 2 MGT Intervals of HAL Traffic at FAST

MGT	TD (CSHA)	Rail Temp (°F) Minimum	Rail Temp (°F) Maximum	Rail Temp (°F) Change
0	12	59	110	51
2	12	53	111	58
4	13	72	220	48
6	24	39	114	75
8	25	58	112	54
10	25	48	109	61
12	28	36	73	37
14	33	40	77	37
16	41	35	99	64
18	41	40	103	63
20	41	61	104	43
22	42	41	93	42

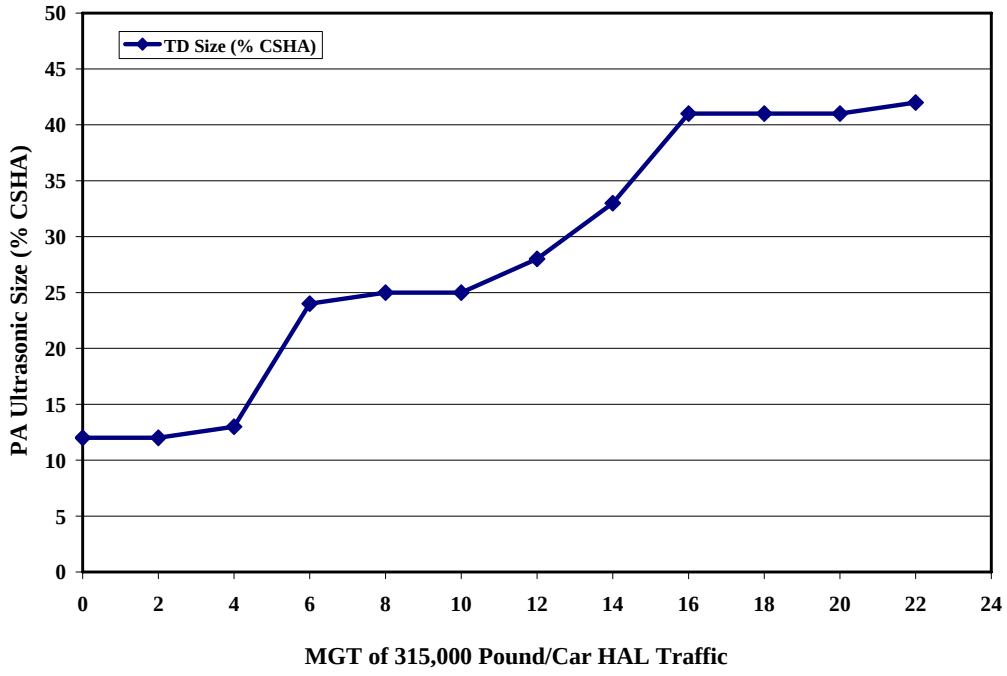

Figure 38. Ultrasonic Flaw Size Growth of the TD in PAS1 Shown in 2 MGT Intervals

The graph shows the greatest flaw size increases at 6 and 16 MGT. These increases in flaw size also correlate with the lowest minimum rail temperature readings of 39 °F and 35 °F (3.9 °C and 1.7 °C). The data also shows the greatest change in rail temperature on these days with a change of 75 °F (23.9 °C) at 6 MGT and 64 °F (17.8 °C) at 16 MGT. This behavior is consistent with findings from research performed and reported in AAR/TTCI report R-963, which documents an increased susceptibility to flaw growth during cold temperatures and large fluctuations in rail temperature (5).

Use of the PA approach to monitor the flaw in PAS1 has demonstrated the sensitivity to accurately size and monitor flaws in track under HAL operations. The approach used in this research effort has also demonstrated that the PA technology can be used not only to size TDs in between train operations but also allows for flaw sizing during train operations over the flaw.

4.0 Conclusions and Recommendations

Characterization of TDs in the railhead has shown that although they are primarily transverse, they can be oriented at a variety of angles. These angles vary significantly from defect to defect, which presents a challenge when inspecting rails for flaws using NDT methods. The PA approaches used during this research effort were chosen to help identify how PA technology might be used to enhance ultrasonic approaches currently used for rail flaw detection of TDs in the railhead. PA technology provides the capability to evaluate the railhead using ultrasonic interrogation from several different angles simultaneously, therefore increasing the probability of detecting and accurately sizing TDs.

Phase I of the research program determined that the ultrasonic PA technology was feasible for use in detecting TDs. The study showed that by using a linear array approach, PA technology was capable of sizing the TD by providing a fairly accurate assessment of the flaw size across the railhead from gage to field. Phase II took this approach a step further by identifying PA probe technologies that would be the most applicable to railhead inspection for the purpose of performing flaw sizing in the field from the side of the railhead. Lastly, in Phase IIA of the research program, the technology was set up in a field environment at FAST and used to monitor TDs during train operations.

Wear causes railhead geometries to continuously change under revenue service operations. These geometry changes can influence the angle at which current conventional ultrasonic approaches inspect the rail. In this study, the transducer was placed on the field side of the railhead, thus reducing the effects of rail wear and surface condition on flaw sizing from rail wear geometry and surface conditions. Current track designs and conditions do not allow for dynamic contact ultrasonic methods to continuously inspect from locations other than at the top (between the gage and field side) of the railhead. Static sizing, however, can be performed at any location of the rail accessible with a contact transducer; and the PA approaches used during this study have shown that TDs can be accurately and rapidly sized from the field side of the railhead using this approach. This finding presents intriguing possibilities for the future of rail flaw detection with the emergence of not only the PA technology but also the potential for combining this technology with conventional, guided wave, laser, air-coupled, and even non-ultrasonic NDT methods.

Continued research into the use of this technology is currently focused on the ongoing monitoring of TDs under HAL operations. It is recommended that this research effort continue in order to optimize the PA probe technologies that can provide the greatest reliability and sensitivity for detecting and sizing of TDs. It is also recommended that research to address the adaptation and incorporation of PA technology into dynamic inspection of rail continue be pursued. This effort will require combining conventional, air-coupled, guided wave, and laser ultrasonic technology with the PA approach. By maturing these technologies to the point where they can dependably supplement each other, it is expected that an increase in rail flaw detection reliability and accuracy, along with an increase in the safety of rail operations, can be achieved.

References

1. *Annual Book of Railroad Statistics*. 1995, 1996, 1997, 1998, 1999, 2000, 2001, 2002, 2003, 2004, 2005. U.S. Department of Transportation, Federal Railroad Administration. Washington, DC.
2. *Draft Rail Defect Manual*. 2006. Committee 4 Rail, Subcommittee-8 Nondestructive Testing of Rail. The American Railway Engineering and Maintenance of Way Association.
3. Granillo, Jesse, Michael Moles. April 2005. *Back to Basics*. "Portable Phased Array Applications." American Society for Nondestructive Testing.
4. American Railway Engineering and Maintenance of Way Association, Chapter 4 Rail, Part 1.1 Recommended Rail Sections. 2005.
5. Garcia, Greg A., et al. July 2003. "Flaw Characterization of Rail Service Failures." Research Report R-963. Association of American Railroads, Transportation Technology Center, Inc., Pueblo, CO.

Acronyms

AAR	Association of American Railroads
AREMA	American Railway Engineering and Maintenance of Way Association
CSHA	cross sectional head area
DDF	Dynamic Depth Focusing
FAST	Facility for Accelerated Service Testing
FRA	Federal Railroad Administration
HAL	heavy axle load
MGT	million gross tons
NDT	nondestructive testing
PA	phased array
RDTF	Rail Defect Test Facility
TD	transverse defect
TOFD	time of flight diffraction
TTCI	Transportation Technology Center, Inc. (the company)
TTC	Transportation Technology Center (the site)